

## Electronic Supplementary Information

### Development of a new flexible nanogenerator from electrospun nanofabric based on PVDF/talc nanosheets composites

Sawan Shetty<sup>1</sup>, Arunjunairaj Mahendran<sup>2</sup>, S. Anandhan<sup>1\*</sup>

<sup>1</sup>Department of Metallurgical and Materials Engineering, National Institute of Technology Karnataka, Srinivas Nagar, Mangaluru-575025, India.

<sup>2</sup>Kompetenzzentrum Holz GmbH, W3C, A-9300 St. Veit/Glan, Klagenfurter Strasse 87-89, Linz, Austria.

\*Correspondence to: S. Anandhan (E-mail:[anandtmg@gmail.com](mailto:anandtmg@gmail.com); [anandhan@nitk.edu.in](mailto:anandhan@nitk.edu.in))



Figure S1 Tensile testing of electrospun fabrics.

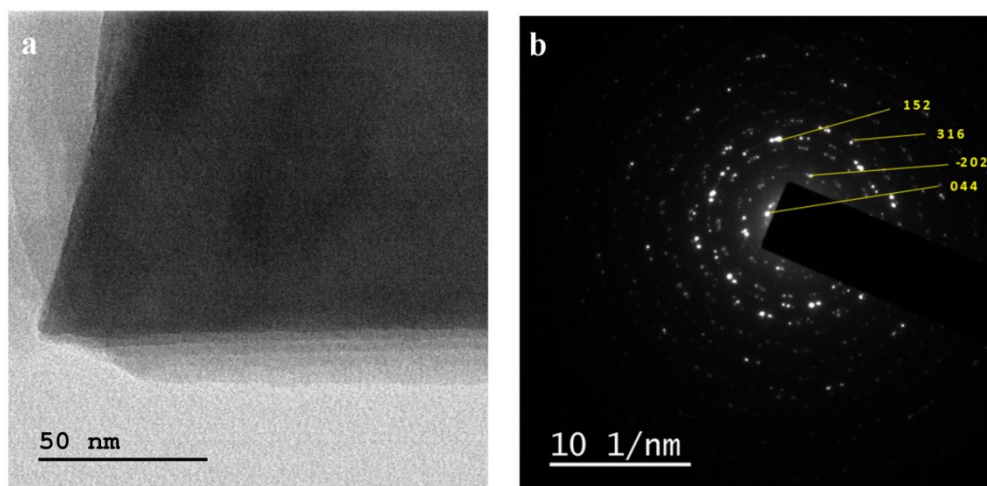
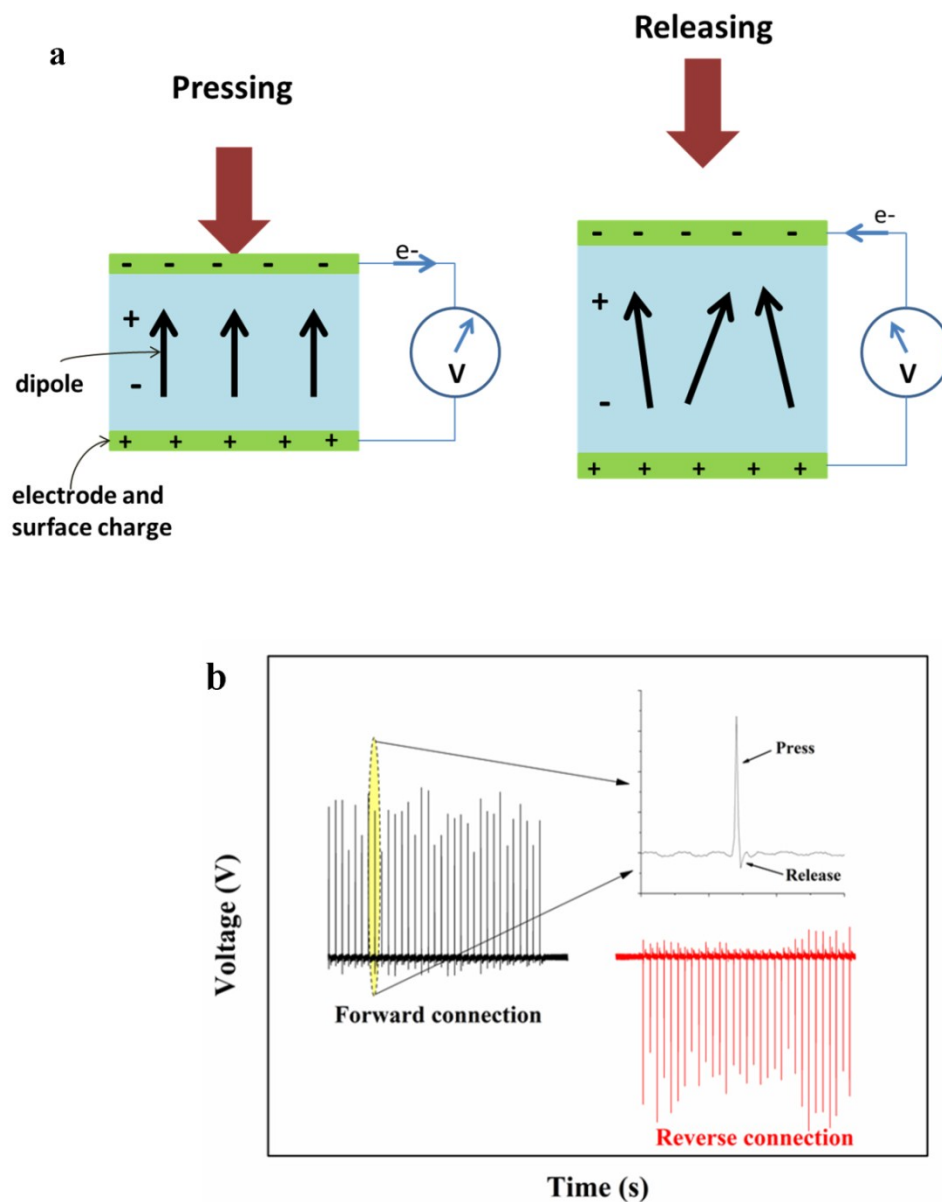


Figure S2 a) TEM image; and b) SAED pattern of talc nanosheets.

### Section S3

When a force is applied to the nanogenerator, the dipoles in the material get orientated along the direction of applied force. This induces potential difference between top and bottom electrodes of the nanogenerator. When the force is released then the electrons flow back to the electrode and produce electrical signal in the opposite direction. Thus, both positive and negative signals are produced under pressing and releasing conditions. The nanogenerator working mechanism and switching polarity test is shown in Figure S3.



**Figure S3** a) Schematic diagram explaining the working mechanism; and b) The switching polarity test of the electrospun nanocomposite fabric based nanogenerator.

#### Section S4

The current response from the talc/PVDF composite nanofabrics was lesser in comparison to the conducting based filler composites, as highlighted in Table S1. This was possibly due to the conducting path provided by the fillers in the matrix.

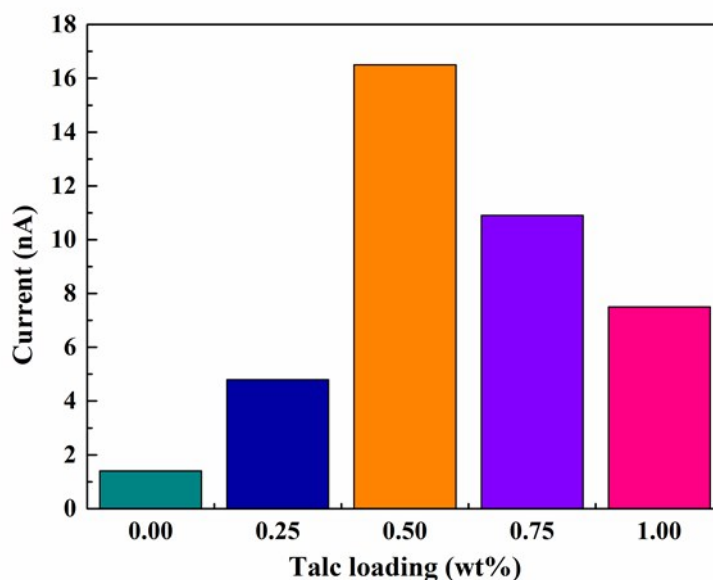


**Figure S4** The output current response of talc/PVDF fabrics based nanogenerator under repetitive tapping mode.

#### Section S5

The nanogenerator is fixed at one end, and the free end is attached to the steel ruler ( $34 \times 2.5 \times 1$  cm) using double-sided adhesive foam tape. The steel ruler scale is linked to a piezoelectric shaker that excites the former. The nanogenerator based on electrospun fabric is deformed mechanically by varying the vibrational frequency of the shaker using a frequency generator. The output response of the nanogenerator under varying frequency modes ( $1 V_{PP}$ , 10 to 50 Hz) is recorded using a data acquisition device interfaced with the computer. Figure S5a and b depict the set-up for frequency modulated-shaker mode.

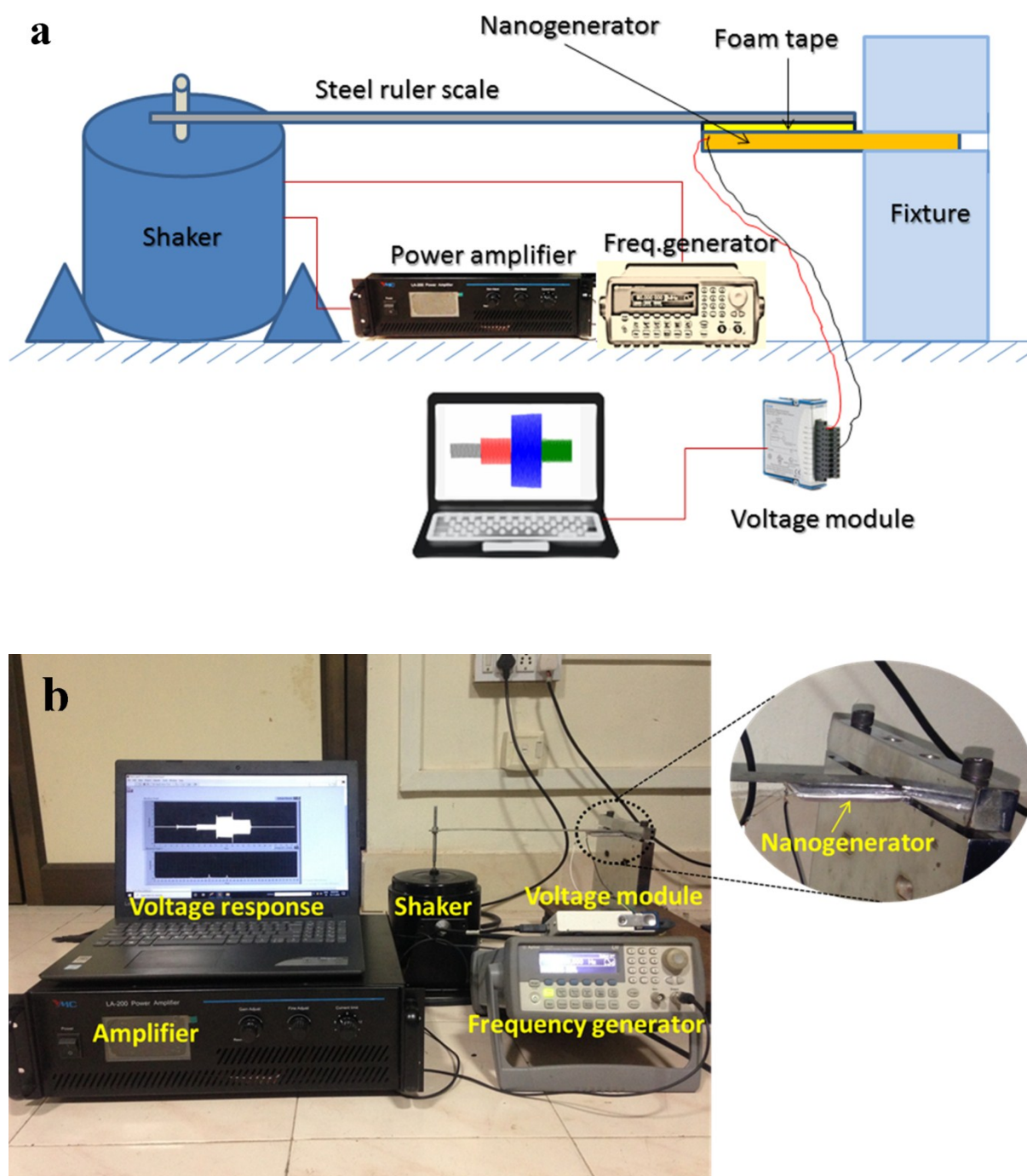


**Figure S5** Illustration of piezoelectric evaluation of E-PVDF and talc/PVDF fabrics based nanogenerator by frequency modulated-shaker mode; (a) Schematic, and (b) Photographic image of the set-up.

**Table S1** Piezoelectric performance comparison between the fabricated nanogenerator and those of PVDF based nanogenerator reported in the literature.

Type of materials	Output Voltage	Output Current	Power Density	Reference
(0.50 wt%) Carbon nanofiber/PVDF nanofibers	5.8 V	1.2 $\mu$ A	-	1
(5 wt%) Potassium sodium niobate/PVDF nanofibers	1.9 V	-	-	2
(0.1 wt%) Graphene/PVDF nanofibers	7.9 V	4.5 $\mu$ A	-	3
Zinc oxide nanorods*/PVDF nanofibers	356 mV	456 nA	-	4
(10 wt%) Potassium sodium niobate/PVDF nanocomposite films	3.4 V	0.1 $\mu$ A	-	5
(20 vol%) Barium titanate/PVDF nanocomposite films	6.7 V	2.4 $\mu$ A	-	6
(2 wt%) Fe-doped reduced graphene oxide/PVDF nanocomposite films	5.1 V	0.254 $\mu$ A	-	7
(16 wt%) Bismuth oxide/PVDF nanocomposite films	3.6 V	2.4 $\mu$ A	1 $\mu$ W**	8
(17.5 wt%) Polyaniline/(10 wt%) halloysite nanotube/PVDF nanofibers	7.2 V	0.75 $\mu$ A	0.25 $\mu$ W/cm <sup>2</sup>	9
Zinc oxide*/PVDF composite fiber membrane	1.12 V	1.6 $\mu$ A	0.2 $\mu$ W/cm <sup>2</sup>	10
(0.50 wt%) Laponite nanoclay/PVDF nanocomposite films	6 V	70 nA	0.63 $\mu$ W/cm <sup>2</sup>	11
<b>(0.50 wt%) talc/PVDF electrospun fabrics</b>	<b>9.1 V</b>	<b>16.5 nA</b>	<b>1.12 <math>\mu</math>W/cm<sup>2</sup></b>	<b>This work</b>

\*Film; \*\*Power

## References

- 1 R. Senthil Kumar, T. Sarathi, K. K. Venkataraman and A. Bhattacharyya, *Mater. Lett.*, 2019, **255**, 126515.
- 2 A. Teka, S. Bairagi, M. Shahadat, M. Joshi, S. Ziauddin Ahammad and S. Wazed Ali,

- Polym. Adv. Technol.*, 2018, **29**, 2537–2544.
- 3 M. M. Abolhasani, K. Shirvanimoghaddam and M. Naebe, *Compos. Sci. Technol.*, 2017, **138**, 49–56.
  - 4 P. Fakhri, B. Amini, R. Bagherzadeh, M. Kashfi, M. Latifi, N. Yavari, S. Asadi Kani and L. Kong, *RSC Adv.*, 2019, **9**, 10117–10123.
  - 5 S. Bairagi and S. W. Ali, *Org. Electron.*, 2019, 105547.
  - 6 P. Hu, L. Yan, C. Zhao, Y. Zhang and J. Niu, *Compos. Sci. Technol.*, 2018, **168**, 327–335.
  - 7 S. K. Karan, D. Mandal and B. B. Khatua, *Nanoscale*, 2015, **7**, 10655–10666.
  - 8 A. Biswas, S. Garain, K. Maity, K. Henkel, D. Schmeißer and D. Mandal, *Polym. Compos.*, 2019, **40**, E265–E274.
  - 9 M. Khalifa, A. Mahendran and S. Anandhan, *Polym. Compos.*, 2019, **40**, 1663–1675.
  - 10 B. Sun, X. Li, R. Zhao, H. Ji, J. Qiu, N. Zhang, D. He and C. Wang, *J. Mater. Sci.*, 2019, **54**, 2754–2762.
  - 11 W. Rahman, S. K. Ghosh, T. R. Middy and D. Mandal, *Mater. Res. Express*, 2017, **4**, 095305.